arXiv:1401.7257v1 [cond-mat.quant-gas] 28 Jan 2014

Isotropic vortex tangles in trapped atomic Bose-Einstein condensates via laser stirring

A. J. Allen, N. G. Parker, N. P. Proukakis, and C. F. Barenghi*
Joint Quantum Centre (JQC) Durham-Newcastle, School of Mathematics and Statistics, Newcastle University, Newcastle upon Tyne, NE1 7RU, England, UK.
(Dated: January 29, 2014)

The generation of isotropic vortex configurations in trapped atomic Bose-Einstein condensates offers a platform to elucidate quantum turbulence on mesoscopic scales. We demonstrate that a laser-induced obstacle moving in a figure-eight path within the condensate provides a simple and effective means to generate an isotropic three-dimensional vortex tangle due to its minimal net transfer of angular momentum to the condensate. Our characterisation of vortex structures and their isotropy is based on projected vortex lengths and velocity statistics obtained numerically via the Gross-Pitaevskii equation. Our methodology provides a possible experimental route for generating and characterising vortex tangles and quantum turbulence in atomic Bose-Einstein condensates.

PACS numbers: 03.75.Kk, 03.75.Lm, 67.85.-d
Keywords: Quantum turbulence, Vortices, Laser-stirring, Bose–Einstein condensates

Vortices in ordinary (classical) fluids, as well as quantum fluids, characterise turbulent flow [1, 2]. Turbulence in classical fluids has been intensely studied in many branches of physics and engineering over a prolonged period. Characterising turbulence and understanding its dynamics is one of the key goals of these fields. Homogeneous, isotropic turbulence is the benchmark to understand vortex dynamics away from boundaries. Quantum fluids, such as superfluid He and atomic Bose-Einstein condensates (BECs), where the circulation is quantized and viscosity is absent, open up the possibility of a context in which to study turbulence which is simpler than in ordinary fluids. Large vortex tangles have been created experimentally in superfluid He for this purpose. The investigation of the properties of such systems has revealed, for certain parameter regimes, the emergence of classical-like behaviour (such as the Kolmogorov scaling [3–5] of the energy spectrum for homogeneous isotropic turbulence) from the dynamics of elementary quantum vortices.

Usually terms like "turbulence" and "vortex tangles" refer to disordered fluid systems containing vortices and eddies in which a huge range of lengthscales and timescales are excited; scaling laws therefore can be identified. Unlike ordinary fluids and superfluid helium, atomic BECs are relatively small, in the sense that there is not a large separation of lengthscales between the vortex core size, the average intervortex separation and the system size [6]. An important question which should be addressed in this context, is whether a relatively small vortex configuration exhibits turbulent properties, or it is simply chaotic. A first step in addressing this question is to demonstrate a technique for generating a few interacting vortices (see Fig. 1 (left)) that give isotropic flow statistics (see Fig. 1 (right)), which is the main result of this paper.

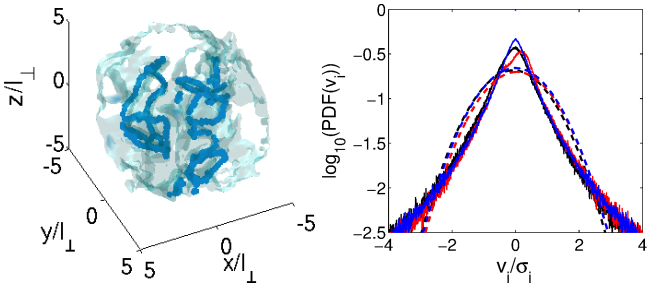

FIG. 1: Tangle of few interacting vortices (left) exhibiting isotropic non-Gaussian flow statistics (right). Left: Density isosurface generated by stirring a spherically symmetric condensate along one plane in a figure-eight path (at time $t \approx t_{\rm stir} = 17.1\omega^{-1}$ when the stirrer has just been removed after approximately two oscillations), with the vortex cores visualised by the dark blue dots. Right: PDFs of velocity components v_x (black), v_y (red) and v_z (blue) at time $t \approx t_{\rm stir}$. The non-Gaussian nature of the turbulent velocity field is made apparent by the large deviation of the PDFs from the corresponding gPDFs, calculated by Eq. (3) (dashed lines).

The experimental realisation of BECs [7–9] has opened up the possibility of experimentally generating a turbulent tangle of vortices in a highly controllable system. Vortex lattices [10–15] and collections of vortex dipoles [16], as well as multiply-charged [17] and multi-component [18–20] vortices can be created, and their two dimensional (2D) column distributions can even be imaged in real-time [21]. With regards to quantum turbulence, a landmark experiment recently generated a small tangle of vortices in a trapped weakly-interacting BEC through the combination of rotation and an external oscillating perturbation [22–24]. Several theoretical works have studied the statistical properties of vortex tangles in three-dimensional (3D) superfluid systems [25–28]. Another proposed method to generate a vortex tangle combines rotations about two different axes [29].

Atomic BECs are typically inhomogeneous because of the harmonic potentials which are used to confine

*Electronic address: carlo.barenghi@ncl.ac.uk

them (although there are ongoing efforts to minimize the effects of inhomogeneity via the creation of 'box-like' condensates [30]); because of the small number of vortices generated, the prevailing vortex configuration is unlikely to be isotropic if it contains only a few vortices. A summary of the features and main unresolved issues in such systems can be found in [6].

It is well known that an obstacle moving through a superfluid will nucleate vortices above a critical speed [31]. In a BEC such an obstacle can be generated via an incident blue-detuned laser beam, which induces a localised repulsive potential through the optical dipole force. Deflection of the laser beam can then be performed to move the obstacle over time. This technique, termed "laser stirring" [15, 32–34], has proven to be an efficient way of generating large numbers of vortices both experimentally [15, 16, 33, 34] and theoretically [32, 35–37]. In particular, laser stirring in a circular path has led to the formation of vortex lattice states [15] due to its imparting of angular momentum to the condensate (the ground state of a superfluid with sufficient angular momentum being a vortex lattice [34, 38, 39]).

In this paper we show that laser stirring in a figure-eight pattern in a two dimensional plane can be used to generate a fully three dimensional isotropic vortex tangle in a trapped BEC, a vortex configuration suitable to study quantum turbulence. While this stirring is an efficient means of generating vortices it imparts minimal angular momentum to the condensate, thus favouring the generation of a tangle of vortices rather than a vortex lattice. Following cessation of the stirring, the tangle decays isotropically. Since velocity statistics [40] and vortex length [38] are routinely used to measure tangle dynamics in He experiments of quantum turbulence, we apply these measures to characterise the vortex dynamics.

Our analysis is based on numerical simulations of the 3D Gross-Pitaevskii equation [39, 41]:

$$i\hbar\frac{\partial\phi(\mathbf{r},t)}{\partial t} = \left(-\frac{\hbar^2}{2m}\nabla^2 + V(\mathbf{r},t) + g|\phi(\mathbf{r},t)|^2 - \mu\right)\phi(\mathbf{r},t), \quad (1)$$

an accurate model for vortical structures in the limit of zero temperature and weak interactions, which describes the condensate by a macroscopic wavefunction $\phi(\mathbf{r},t)$. This equation is commonly expressed hydrodynamically using a transformation of the form $\phi(\mathbf{r},t) = |\phi(\mathbf{r},t)|e^{i\theta(\mathbf{r},t)}$, where $\theta(\mathbf{r},t)$ is the phase and the superfluid velocity is identified as $\mathbf{v}(\mathbf{r},t) = (\hbar/m)\nabla\theta(\mathbf{r},t)$. The interatomic interactions are parametrized by $g = 4\pi\hbar^2 a_s/m$, where a_s is the $s-$wave scattering length and μ is the condensate chemical potential. The external potential acting on the BEC is of the form $V(\mathbf{r},t) = m\omega^2 r^2/2 + V_\mathrm{l}(x,y,t)$. The first term represents a spherically symmetric harmonic trap, of frequency ω, used to confine the gas. The second term represents a Gaussian time-dependent laser-induced potential, uniform along z:

$$V_\mathrm{l}(x,y,t) = V_0\mathrm{exp}\left[-\frac{(x-x_l(t))^2 + (y+y_l(t))^2}{d^2}\right]. \quad (2)$$

The amplitude V_0 is proportional to the intensity of the stirring laser beam [39, 42], $x_l(t)$ and $y_l(t)$ are the positions of the center of the stirrer at time t, and d is the beam's width. For a figure-eight stirring path, the time dependent coordinates of the obstacle are given by $(x_l(t), y_l(t)) = (x_0\cos(\nu_l t)(1-\sin(\nu_l t)), y_0\cos(\nu_l t)\sin(\nu_l t))$, where $x_0 = y_0 = 4l_\perp$ and $\nu_l = 0.74(\omega/2\pi)$ is the angular frequency of the moving obstacle. We solve Eq. (1) on a 300^3 grid [48] with $g = 16000 l_\perp\hbar\omega$, where $l_\perp = \sqrt{\hbar/m\omega}$ is the harmonic oscillator length, and $\mu = 30\hbar\omega$. For a trapping frequency of $\omega = 2\pi\times 150$ Hz this corresponds to approximately $21,000$ ^{87}Rb atoms. All results presented in this paper will be expressed in these units. We choose an obstacle with fixed width ($d = l_\perp/2$) and slowly increase its amplitude V_0 linearly with time ($V_0 = 1.5t$) until it reaches a maximum value at the time where it is removed; in this way disruptive shock waves are minimized. The total stir time is $t_\mathrm{stir} = 17.1\omega^{-1}$, by which point the beam has undergone almost two full oscillations of the figure-eight path (see the left inset of Fig. 3 (bottom)) and V_0 has reached its maximum value of $\approx 25.7\hbar\omega$.

Our figure-eight stirring path minimizes the net transfer of angular momentum to the condensate, in comparison to the circular path which imparts angular momentum around the stirring axis and results in an ordered array of vortices arranged in a lattice configuration [10, 11, 13, 15]. An added advantage to the figure-eight path is that the obstacle generates a range of vortex lengths through the whole extent of the condensate (across varying axial width), allowing for more bending and tangling of vortex lines than the simpler circular stirring. During the stirring, vortices are nucleated by the obstacle and form a wake behind it. When the obstacle is removed at time $t = t_\mathrm{stir}$, what is left is a tangle of reconnecting vortices, as shown in Fig. 1 (left) [49]. The surface of the condensate (spherical when unperturbed) is made uneven by large density waves created by the obstacle and by the motion and reconnections of vortices [43].

It is difficult to determine by visual inspection how isotropic a vortex tangle is [28]. To measure it precisely, we compute the probability density function (normalised histogram, or PDF for short) of the velocity components v_x, v_y and v_z. The velocity is computed directly from the definition $\mathbf{v}(\mathbf{r}) = (\phi^*\nabla\phi - \phi\nabla\phi^*)(2i|\phi|^2)$.

Figure 1 (right) shows such PDFs just after the stirrer has been removed. The good overlap of these velocity PDFs confirms the isotropy of the turbulent velocity field. Moreover, the high degree of symmetry for the PDFs about $v = 0$ confirms that negligible linear momentum is imparted in all directions. For comparison, we also include the Gaussian PDF (gPDF) of each velocity

component (correspondingly colored dashed lines), given by

$$\mathrm{gPDF}(v_i) = \frac{1}{\sigma_i\sqrt{2\pi}}\exp\left(\frac{-(v_i-\tilde{\mu}_i)^2}{2\sigma_i^2}\right), \qquad (3)$$

where σ_i and $\tilde{\mu}_i$ are the standard deviation and the mean. Figure 1 (right) thus also confirms the non-Gaussian (hence non-classical) nature of the velocity PDFs due to the quantised nature of the vortices [5, 28, 40, 44].

We have also considered (see Fig. 2) the velocity PDFs for a straight vortex (left) as well as a vortex ring (right). In addition to the non-Gaussian nature, these reveal non-isotropic velocity PDFs, hence substantiating our claim about the importance of the isotropy of our generated tangle in Fig. 1 (left). Although the tangle shown in Fig. 1 contains relatively few vortices, the resulting velocity distribution shown in Fig. 1 (right) resembles the isotropic velocity distributions of a dense vortex tangle in superfluid helium [45].

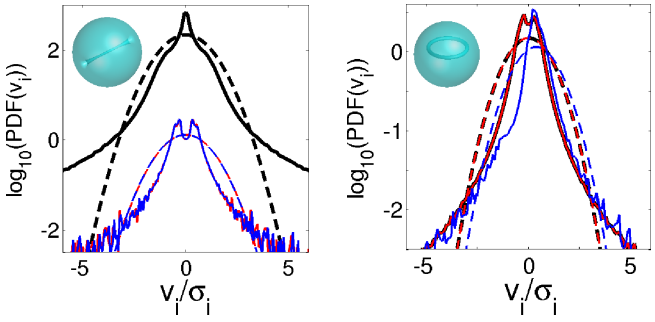

FIG. 2: PDFs of velocity components v_x (black), v_y (red) and v_z (blue) of a single vortex line oriented in the $y-z$ direction (left) and a vortex ring in the $x-y$ plane (right). Insets show corresponding isosurfaces of the condensate density.

A further measure to assess isotropy (also routinely used in turbulent superfluid He systems) [38] is based on projected line length L_x, L_y and L_z in the x, y and z-directions. An isotropic vortex configuration will have $L_x/L \approx L_y/L \approx L_z/L$ where the total line length L. To determine the vortex length, we find all grid cells where the density has a minimum and the phase around that grid point changes by 2π. We restrict the calculation to within 78% of the Thomas-Fermi radius $R_{\rm TF} = \sqrt{2\mu}\,l_\perp$ to avoid artefacts arising from the low density edge of the condensate.

Figure 3 (top and intermediate) give condensate density and phase slices (at $z = 0$) during the stirring ($t < t_{\rm stir}$, (A)), just after removing the stirrer ($t \approx t_{\rm stir}$, (B)) and at a much later time (C). Singularities in the phase plot indicate the presence of a vortex; the charge of a vortex can be inferred from the direction of the phase winding with both positive and negatively charged vortices present in these images. Additionally, these phase plots indicate the presence of nonlinear waves in this system, confirming that this stirring mechanism produces a highly disturbed velocity field. In C, the

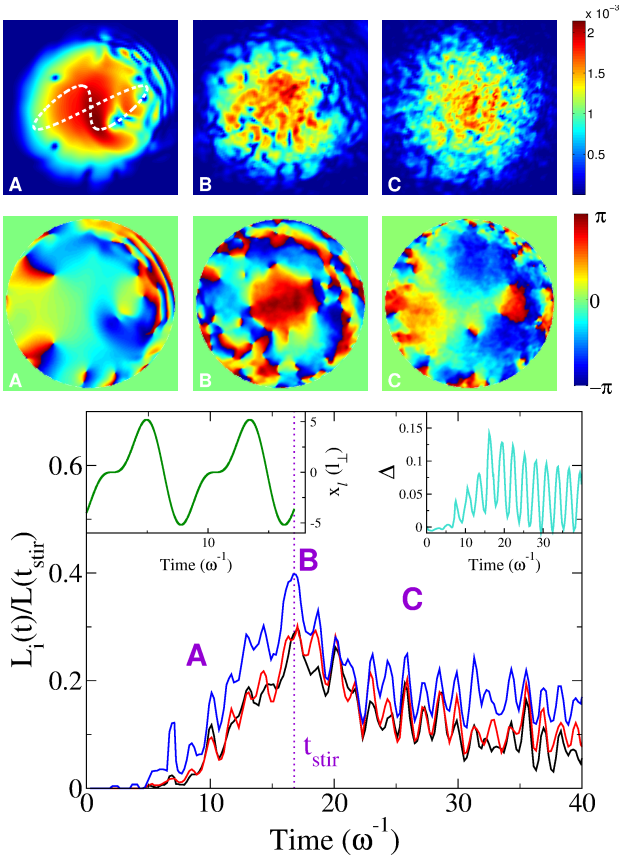

FIG. 3: (Color online) Top: Density images of the condensate at $z = 0$ and $x, y = [-8, 8]l_\perp$ at times $\omega t = 9.1$ (A) and 17.1 (B) and 24.9 (C) (also marked on the lower graph where (B) refers to the snapshot from Fig. 1 at time $t = t_{\rm stir}$). Regions of high (brown/red) and low (blue) density are apparent as indicated by the colorbar. Density is measured in units of $l_\perp^{-3}$. The figure-eight path of the obstacle is shown by the white dashed line in (A). Intermediate: Corresponding phase snapshots. Singly charged vortices correspond to 2π phase singularities. To avoid phase artefacts at very low density, the phase is truncated beyond $R_{\rm TF}$. Bottom: Measured projected vortex lengths L_i, vs. time in the x (black), y (red) and z (blue) directions. Inset (left): Trajectory of laser in $x-$direction, x_l, up to time $t_{\rm stir}$. Inset (right): The displaced density Δ versus time, where the displaced density is the difference in the norm between a condensate containing no vortices, ϕ_1, and the stirred condensate, ϕ_2, i.e. $\Delta = \int_{\mathcal{V}} |\phi_1|^2 dV - \int_{\mathcal{V}} |\phi_2|^2 dV$, where $\mathcal{V} = (4\pi/3)R_{\rm cut}^3$, with $R_{\rm cut} = 0.78R_{\rm TF}$.

tangle is less dense than in A and B as most of the vortices have decayed to the edge of the condensate. The bottom part of the figure shows the corresponding projected vortex lengths. Following a near uniform increase of L during stirring ($t < t_{\rm stir}$), all vortex lengths L_x, L_y and L_z decay together after the stirrer has been removed ($t > t_{\rm stir}$), indicating that the vortex configuration maintains a high degree of isotropy during its decay. This is further confirmed by inspection of the velocity PDFs at later times (see Fig. 4).

Figure 3 also shows that during the decay of L, all

three directional projections oscillate. This is an artifact of the method for calculating the vortex length, which measures it within a fixed spherical volume, $(4\pi/3)R_{\rm cut}^3$, where $R_{\rm cut} = 0.78R_{\rm TF}$. The entire condensate undergoes volume oscillations [28], and vortices move in and out of the region where the length is determined. The dominant frequency of this linelength oscillation is approximately 2.2ω which is close to the frequency of the monopole mode ($\omega_{osc} = \sqrt{5}\omega$ in the TF approximation [50]) of a harmonically-trapped BEC [39, 41]. It is worth remarking that the widths of the condensate in all three directions oscillate in phase with each other, in agreement with the excitation of this mode [51]. Further analysis shows that the magnitude of these oscillations increase with stir time.

In order to relate vortex linelength to an experimentally observable quantity, such as volume, we also measure the norm in the measurement volume $(4\pi/3)R_{\rm cut}^3$ and compare this to a condensate of the same total atom number containing no vortices - see the right inset of Fig. 3 (bottom). During the stirring, we find that as the linelength increases, the displaced density also increases, with both decreasing when the stirrer is removed. The displaced density additionally undergoes oscillations and these are found to be of the same frequency as those of the vortex length. Since the total atom number remains constant, we infer that the volume of the condensate increases to accommodate the vortices. This effect is visible experimentally [46] and can monitored by measuring the atom number within a specified radius of the BEC [47].

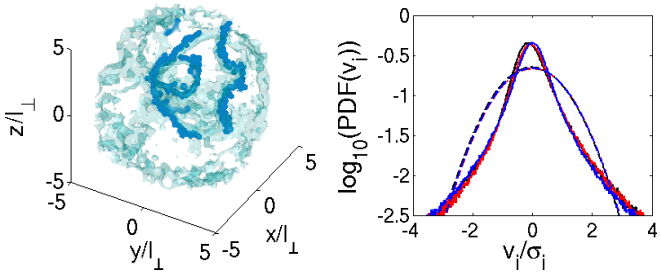

FIG. 4: (Color online) Left: Density isosurface at time $\omega t = 25.7$ (as in Fig. 1) showing a few remaining vortices during the decay of the dense vortex tangle. Right: Corresponding velocity PDFs for components v_x (black), v_y (red) and v_z (blue) (as in Fig. 1).

In conclusion, we have proposed a novel stirring protocol in ultracold atomic gases, aimed at generating an isotropic vortex tangle. Unlike the usual circular path of stirring (which eventually leads to an ordered vortex lattice), and linear sweeping (which generates vortex dipoles and can be expected to heavily excite the condensate dipole mode), stirring a spherical condensate along a planar figure-eight path, via a laser-induced obstacle aligned along a given axis, results in the generation of an isotropic vortex tangle. Cessation of the stirring leads to the subsequent isotropic decay of the tangle. As such, this stirring protocol represents an efficient route to experimentally generate dense isotropic vortex tangles in trapped Bose-Einstein condensates and is a further step towards efficient generation of quantum turbulence in these systems.

We gratefully acknowledge A. C. White for many useful discussions. AJA, NPP and CFB acknowledge funding from the EPSRC (Grant number: EP/I019413/1).

[1] U. Frisch, *Turbulence. The legacy of A.N. Kolmogorov.* (Cambridge University Press, 1995).
[2] C. Barenghi, R. Donnelly, W. Vinen, and eds., *Quantized Vortex Dynamics and Superfluid Turbulence* (Springer, Berlin, 2001).
[3] J. Maurer and P. Tabeling, EPL (Europhysics Letters) **43**, 29 (1998).
[4] J. Salort, C. Baudet, B. Castaing, B. Chabaud, F. Daviaud, T. Didelot, P. Diribarne, B. Dubrulle, Y. Gagne, F. Gauthier, et al., Physics of Fluids **22**, 125102 (2010).
[5] C. Barenghi, V. L'vov, and P.-E. Roche (2013), arXiv:1306.6248 [cond-mat.other].
[6] A. J. Allen, N. G. Parker, N. P. Proukakis

and C. F. Barenghi, (2013), arXiv:1302.7176 [cond-mat.quant-gas].
[7] M. H. Anderson, J. Ensher, M. R. Matthews, and C. E. Wiemann, Science **269**, 198 (1995).
[8] K. B. Davis, M. O. Mewes, M. R. Andrews, N. J. van Druten, D. S. Durfee, D. M. Kurn, and W. Ketterle, Phys. Rev. Lett. **75**, 3969 (1995).
[9] C. C. Bradley, C. A. Sackett, J. J. Tollett, and R. G. Hulet, Phys. Rev. Lett. **79**, 1170 (1997).
[10] K. W. Madison, F. Chevy, W. Wohlleben, and J. Dalibard, Phys. Rev. Lett. **84**, 806 (2000).
[11] E. Hodby, G. Hechenblaikner, S. A. Hopkins, O. M. Maragò, and C. J. Foot, Phys. Rev. Lett. **88**, 010405 (2001).
[12] J. R. Abo-Shaeer, C. Raman, and W. Ketterle, Phys. Rev. Lett. **88**, 070409 (2002).
[13] J. R. Abo-Shaeer, C. Raman, J. M. Vogels, and W. Ketterle, Science **292**, 476 (2001).
[14] K. W. Madison, F. Chevy, V. Bretin, and J. Dalibard, Phys. Rev. Lett. **86**, 4443 (2001).
[15] C. Raman, J. R. Abo-Shaeer, J. M. Vogels, K. Xu, and W. Ketterle, Phys. Rev. Lett. **87**, 210402 (2001).
[16] T. W. Neely, E. C. Samson, A. S. Bradley, M. J. Davis, and B. P. Anderson, Phys. Rev. Lett. **104** 160401 (2010).
[17] Y. Shin, M. Saba, M. Vengalattore, T. A. Pasquini, C. Sanner, A. E. Leanhardt, M. Prentiss, D. E. Pritchard, and W. Ketterle, Phys. Rev. Lett. **93**, 160406 (2004).
[18] M. R. Matthews, B. P. Anderson, P. C. Haljan, D. S. Hall, C. E. Wieman, and E. A. Cornell, Phys. Rev. Lett. **83**, 2498 (1999).
[19] B. P. Anderson, P. C. Haljan, C. E. Wieman, and E. A. Cornell, Phys. Rev. Lett. **85**, 2857 (2000).
[20] V. Schweikhard, I. Coddington, P. Engels, S. Tung, and E. A. Cornell, Phys. Rev. Lett. **93**, 210403 (2004).
[21] D. V. Freilich, D. M. Bianchi, A. M. Kaufman, T. K. Langin, and D. S. Hall, Science **329**, 1182 (2010).
[22] E. A. L. Henn, J. A. Seman, G. Roati, K. M. F. Magalhães, and V. S. Bagnato, Phys. Rev. Lett. **103**, 045301 (2009).
[23] J. Seman, E. Henn, R. Shiozaki, G. Roati, F. Poveda-Cuevas, K. Magalhes, V. Yukalov, M. Tsubota, M. Kobayashi, K. Kasamatsu, et al., Laser Physics Letters **8**, 691 (2011).
[24] R. Shiozaki, G. Telles, V. Yukalov, and V. Bagnato, Laser Physics Letters **8**, 393 (2011).
[25] C. Nore, M. Abid, and M. E. Brachet, Physics of Fluids **9**, 2644 (1997).
[26] N. G. Berloff and B. V. Svistunov, Phys. Rev. A **66**, 013603 (2002).
[27] J. Yepez, G. Vahala, L. Vahala, and M. Soe, Phys. Rev. Lett. **103**, 084501 (2009).
[28] A. C. White, C. F. Barenghi, N. P. Proukakis, A. J. Youd, and D. H. Wacks, Phys. Rev. Lett. **104**, 075301 (2010).
[29] M. Kobayashi and M. Tsubota, Phys. Rev. A **76**, 045603 (2007).
[30] A. L. Gaunt, T. F. Schmidutz, I. Gotlibovych, R. P Smith and Z. Hadzibabic, Phys. Rev. Lett. **110**, 200406 (2013).
[31] T. Frisch, Y. Pomeau, and S. Rica, Phys. Rev. Lett. **69**, 1644 (1992).
[32] B. M. Caradoc-Davies, R. J. Ballagh, and K. Burnett, Phys. Rev. Lett. **83**, 895 (1999).
[33] C. Raman, M. Köhl, R. Onofrio, D. S. Durfee, C. E. Kuklewicz, Z. Hadzibabic, and W. Ketterle, Phys. Rev. Lett. **83**, 2502 (1999).
[34] G. P. Kevrekidis, D. J. Frantzeskakis, R. Carretero-Gonzlez (Eds.), *Emergent Nonlinear Phenomena in Bose-Einstein Condensates, Theory and Experiment* (Springer Series on Atomic, Optical, and Plasma Physics, Vol. 45, 2008).
[35] A. C. White, C. F. Barenghi, and N. P. Proukakis, Phys. Rev. A **86**, 013635 (2012).
[36] M. T. Reeves, B. P. Anderson, and A. S. Bradley, Phys. Rev. A **86**, 053621 (2012).
[37] M. T. Reeves, T. P. Billam, B. P. Anderson, and A. S. Bradley, Phys. Rev. Lett. **110**, 104501 (2013).
[38] R. J. Donnelly, *Quantized Vortices in Helium II* (Cambridge Univ. Press, Cambridge, 1991).
[39] C. J. Pethick and H. Smith, *Bose-Einstein condensation in dilute gases* (Cambridge University Press, 2002).
[40] M. S. Paoletti, M. E. Fisher, K. R. Sreenivasan, and D. P. Lathrop, Phys. Rev. Lett. **101**, 154501 (2008).
[41] L. P. Pitaevskii and S. Stringari, *Bose-Einstein Condensation* (Oxford University Press, Great Clarendon Street, Oxford, 2003).
[42] C. S. Adams and E. Riis, Progress in Quantum Electronics **21**, 1 (1997).
[43] S. Zuccher, M. Caliari, A. W. Baggaley, and C. F. Barenghi, Physics of Fluids **24**, 125108 (2012).
[44] M. S. Paoletti, and D. P. Lathrop, Ann. Rev. Cond. Matt. Phys. **2**, 213 (2011).
[45] A. W. Baggaley, and C. F. Barenghi, Phys. Rev. E **84**, 067301 (2011).
[46] V. S. Bagnato, *Private communication.*
[47] G.-B. Jo, J.-H. Choi, C. A. Christensen, T. A. Pasquini, Y.-R. Lee, W. Ketterle, and D. E. Pritchard, Phys. Rev. Lett. **98**, 180401 (2007).
[48] We solve Eq. (1) numerically using a 4th order Runge Kutta (Error = $O(\Delta t^4)$) on a discrete grid with spatial step $\Delta x = \Delta y = \Delta z = 0.1 l_\perp$, and time step $\Delta t = 0.001\omega^{-1}$.
[49] See time evolution of isosurfaces in the Supplemental Material provided.
[50] It is interesting to note that the signature of this mode appears clearly (and only slightly shifted from the true monopole mode frequency) from a random configuration of vortices, in agreement with R.P. Teles *et al.* Phys. Rev. A 88, 053613 (2013) for a single vortex in the centre of a harmonically trapped condensate.
[51] We also see evidence of a second frequency appearing which is an exact multiple of the first.